Endoplasmic reticulum regulation of glucose metabolism in glioma stem cells

MARÍA TUROS-CABAL[1-3], ANA M. SÁNCHEZ-SÁNCHEZ[1-3], NOELIA PUENTE-MONCADA[1-3], FEDERICO HERRERA[4,5], JEZABEL RODRIGUEZ-BLANCO[6,7], ISAAC ANTOLIN[1-3], MARCO ANTONIO ALVAREZ-VEGA[2,3,8], CARMEN RODRÍGUEZ[1-3] and VANESA MARTÍN[1-3]

[1]Morphology and Cellular Biology Department, Faculty of Medicine; [2]Oncology Institute of Principality of Asturias (IUOPA), University of Oviedo, Oviedo 33006; [3]Health Research Institute of Principality of Asturias (ISPA), Avenida Hospital University, 33011 Oviedo, Spain; [4]Department of Chemistry and Biochemistry (DQB); [5]BioISI-Biosystems and Integrative Sciences Institute, Faculty of Sciences, University of Lisbon, Lisbon 1749-016, Portugal; [6]Darby Children's Research Institute, Department of Pediatrics; [7]Hollings Cancer Center, Medical University of South Carolina, Charleston, SC 29425, USA; [8]Neurosurgery Department, Central Hospital of Asturias (HUCA), 33011 Oviedo, Spain

Received April 27, 2023; Accepted October 9, 2023

DOI: 10.3892/ijo.2023.5589

Abstract. Glioblastoma (GBM) treatment is extremely challenging due to the high complexity of the tumor. It is one of the tumors in which a subpopulation of highly resistant glioma initiating cells (GICs) has been clearly identified. Thus, understanding the differences between GICs and tumor bulk cells is therefore essential to move to less conventional but more efficient approaches. It was found that, unlike their differentiated progeny, GICs survival and maintenance of stem cell properties depend on mitochondrial metabolism. GICs present higher glucose uptake and mitochondrial membrane potential and reduced lactate dehydrogenase activity, being more sensitive to mitochondrial inhibition than their differentiated counterparts. Calcium flux to the mitochondria appears to play an essential role in the maintenance of this distinct metabolic phenotype with a decrease in the expression of voltage-dependent anionic channel (VDAC) and Grp75, two of the proteins of the IP3R-Grp75-VDAC complex that transfers calcium from the endoplasmic reticulum (ER) to the mitochondria. Disruption of ER homeostasis using ER stress inducers or inhibition of ER-mitochondrial contact sites using the Grp75 inhibitor MKT-077 resulted in cytotoxicity of GICs and loss of stemness. Moreover, MKT-077 also potentiates the effect of temozolomide, current treatment for glioblastoma. In summary, the present data indicated that ER-mitochondrial homeostasis is essential for regulation of GICs glucose metabolism and survival.

Correspondence to: Dr Vanesa Martin, Morphology and Cellular Biology Department, Faculty of Medicine, University of Oviedo, 6 Julian Claveria Road, 33006 Oviedo, Spain
E-mail: martinvanesa@uniovi.es

Key words: glioma initiating cells, metabolic reprograming, endoplasmic reticulum, mitochondria, mitochondria-ER contact sites

Introduction

Glioblastoma (GBM), the most frequent and most lethal primary malignant brain tumor, represents a highly complex tumor consisting in cancer cells and various non-neoplastic cells (1,2). This complexity represents a challenge to achieve an effective therapy to overcome the current median survival of 14 months even after conventional therapy which combines surgical resection, radiotherapy and chemotherapy (3). Additionally, GBM is one of the tumors in which a subpopulation of cancer initiating cells with properties of stem cells has been clearly identified. This glioma initiating cells (GICs) and their differentiated counterpart (tumor bulk cells) may represent opposite extremes of cells forming the highly heterogenous GBM mass *in vivo* (4,5). GICs not only resist current treatments and repopulate the tumor but are also able to evade the host immune system. Thus, the greater proportion of GICs, the higher tumor aggressivity and poorer prognosis (6), as current therapies show poor efficacy against GICs (4,6). For these reasons, understanding the differences between both types of cancer cells and the heterogenicity of the tumor could help to move cancer therapy towards less conventional but more efficient approaches.

It must also be considered that the subpopulation of cancer stem cells (CSCs) is not 'immovable' and that new stem cells may appear depending on multiple factors. Evidence suggests that stem cell properties can be acquired as a consequence of mutations and metabolic changes occurring in normal stem cells or differentiated cancer cells that move up the cancer cell hierarchy for their expression of pluripotent genes. In this sense, numerous of the identified CSCs' biomarkers have some role in cellular metabolism. These metabolic changes, capable

of inducing CSCs reprogramming are collectively called 'metabo-stemness' (7).

Loss of control of mitochondrial metabolism is one of the main hallmarks of cancer (8). Numerous tumor cells, including GBM, have an altered glucose metabolism known as Warburg effect (9), which favors the transformation of pyruvate to lactate instead of its incorporation into the tricarboxylic acid cycle and the subsequent electron transport chain (ETC) in the mitochondria. This metabolic adaptation, although it is energetically less favorable, has other advantages for tumor cells in terms of redox balance and synthesis of intermediate metabolites (10). However, while Warburg effect has been described for GBM, data appear to indicate that metabolism could vary between different tumor populations and can be also modulated within same tumor population by tumor microenvironment (11). Thus, a previous study showed that GICs are less glycolytic than differentiated glioma cells (12). But on the other hand, there is also abundant literature that supports aerobic glycolysis as the main bioenergetic source in CSCs of various tumor types including GBM (13).

Moreover, it has been also described that glycolysis does not account for the total production of ATP in GBM, suggesting the role of other metabolic routes (9) such as beta oxidation of fatty acids in the mitochondria (14) that requires the endoplasmic reticulum (ER) participation too. ER plays a central role in regulation of the adaptative response needed for a tumoral cell in order to survive to the hostile microenvironment generated as a consequence of the high proliferation rate that includes oxidative stress, nutrient and lipid deprivation and hypoxia (15). Although the mitochondria and ER were classically considered to function independently, electron microscopy ultrastructural studies already described points of great proximity between the two organelles that made researchers suspect an interrelation between them. These points, known as mitochondria-ER contact sites (MERCS) are sites of close proximity between both organelles where several different proteins are recruited. Among these proteins is the mitochondrial membrane voltage-dependent anionic channel (VDAC) that interacts with the inositol trisphosphate receptor (IP3R) of the ER through the chaperone GPR75, being responsible for the transfer of calcium from the ER to the mitochondria (16). This calcium is essential for the activity of dehydrogenases of the Krebs cycle, the production of energy and consequently cell survival (17). Of interest, a previous electron microscopy ultrastructural study has described differences at the level of MERCS between GICs and differentiated tumor cells (18), suggesting an important role of ER-mitochondria interactions in the biology of GBM cells.

It was hypothesized that there are differences at the level of ER and mitochondrial functionality between GICs and their differentiated counterparts that plays a central role in regulation of glucose metabolism and that these differences are key to maintaining the glioma stem cell subpopulation.

Materials and methods

Cell culture and reagents. Neurospheroid cultures were established from acute cell dissociation of human GBM post-surgical specimens and maintained in DMEM/F12 medium supplemented with B27 and N2 (Invitrogen; Thermo Fisher Scientific, Inc.) plus EGF and bFGF (20 ng/ml each; MilliporeSigma) according to the previously described procedures (19,20). Neurospheroid cultures display a GICs phenotype (self-renewal, proliferation, expression of stem cell markers, pluripotency and ability to form tumors *in vivo*). For differentiation of GICs, neurospheroids were dissociated using accutase™ (Invitrogen; Thermo Fisher Scientific, Inc.) and seeded in serum DMEM/F12 supplemented with 10% fetal bovine serum (FBS) for 10 days. Culture cells were maintained at 37˚C in a humidified atmosphere of 5% CO_2. The present study was conducted in accordance with the Declaration of Helsinki and was approved (approval no. 2021.008; approved on January 22nd, 2021) by the Clinical Research Ethics Committee of the Principality of Asturias (Oviedo, Spain). Written informed consent was obtained by all patients who participated in the present study.

Cell culture reagents were purchased from MilliporeSigma except for FBS, which was obtained from GIBCO (Invitrogen; Thermo Fisher Scientific, Inc.). Culture flasks and dishes were acquired from Thermo Fisher Scientific, Inc. All other reagents were purchased from MilliporeSigma, unless otherwise indicated.

Compound concentrations used for the experiments were as follows: 20 mM oxamate (cat. no. O2751; Sigma-Aldrich; Merck KGaA), 500 nM rotenone (cat. no. R8875; Sigma-Aldrich; Merck KGaA), 10 μM BAPTA/AM (cat. no. sc-202488; Santa Cruz Biotechnologies, Inc.), 5 μM thapsigargin (cat. no. 586005; Sigma-Aldrich; Merck KGaA), 500 ng/ml tunicamycin (cat. no. sc-3506; Santa Cruz Biotechnologies, Inc.), 1 μM MKT-077 (cat. no. M5449; Sigma-Aldrich; Merck KGaA) and 1-10 μM temozolomide (cat. no. 16437308; Thermo Fisher Scientific, Inc.).

Self-renewal assessment. Self-renewal was determined by the limiting dilution assay, which indicates the number of cells from a primary NS that are needed to form a secondary NS. For this experiment, primary neurospheres were treated overnight with different drugs and then counted with an automatic cell counter and seeded in 96-well plates at dilutions that ranged from 100 cells/well to 1 cell/well. After 7 days of culture, each well was examined for the formation of tumor spheres. Data were analyzed using the web-based tool 'ELDA' (extreme limiting dilution analysis) (http://bioinf.wehi.edu.au/software/elda/).

Evaluation of cell viability. Cell death was determined by means of Trypan blue exclusion assay. Trypan blue uptake is indicative of irreversible membrane damage preceding cell death, giving as a result a blue staining in non-viable cells. For these assays, cells were seeded in 12-well plates at a density of 10^4 cells/ml. After treatments, cells were harvested and resuspended in 400 μl of PBS and 100 μl of 0.4% (w/v) trypan blue solution. The number of cells and the percentage of viable and non-viable cells were determined using an automatic cell counter (Countess™ 3, Invitrogen; Thermo Fisher Scientific, Inc.).

For drug combination studies, cell viability was evaluated using a colorimetric assay, 3-(4, 5-dimethylthiazol-2-yl)-2,5-diphenyltetrazolium bromide (MTT). Briefly, cells were seeded

onto 96-well plates and once the treatments were completed, 10 μl of a MTT solution in PBS (5 mg/ml) w added. After 4 h of incubation at 37˚C, one volume of the lysis solution [sodium dodecyl sulphate (SDS) 20% and dimethylformamide pH 4.7, 50%] was added. The mixture was incubated at 37˚C overnight and the samples were measured in an automatic microplate reader (μQuant; Bio-Tek Instruments, Inc.) at the wavelength of 540 nm. It must be taken into account that none of these protocols allow the determination of the exact mechanism of cell death.

Measurement of glucose uptake using 2-NBDG. Glucose uptake activity was measured using a fluorescent D-glucose analogue 2-[N-(7-nitrobenz-2-oxa-1,3-diazol-4-yl) amino]-2-deoxy-D-glucose (2-NBDG). Cells were seeded in six-well plates at a density of 10^4 cells/ml and treated with the different compounds for 24 h. After treatments, cells were collected and incubated with 10 μM 2-NBDG for 35 min. Fluorescence was measured in a microplate fluorimeter FLX-800 (Bio-Tek Instruments, Inc.) at an excitation wavelength of 467 nm and an emission wavelength of 542 nm. The obtained fluorescence was normalized with total number of cells determined using an automatic cell counter (Countess™ 3).

Determination of mitochondrial calcium levels. Cells were seeded in six-well plates at a density of 10^4 cells/ml. After treatments, cells were collected and incubated with a fluorescent probe specific for mitochondrial Ca^{2+} [3 μM Rhod-2 AM] for 30 min at 37˚C. The fluorescence signal from these cells was measured using a microplate fluorimeter FLX-800 (Bio-Tek Instruments, Inc.) at an excitation and emission wavelength of 552 and 581 nm, respectively. The obtained fluorescence was normalized with total number of cells using an automatic cell counter (Countess™ 3).

Evaluation of mitochondrial membrane potential. The fluorescent probe Rhodamine 123 was used to monitor the electrochemical gradient in mitochondria ($\Delta\Psi$m). Cells were seeded in six-well plates at a density of 10^4 cells/ml and treated with the different compounds for 24 h. After treatments, cells were collected and incubated with 1 μg/ml Rhodamine 123 in serum-free medium for 30 min at 37˚C. Fluorescence was measured using a microplate fluorimeter FLX-800 (Bio-Tek Instruments, Inc.) at an excitation and emission wavelength of 488 and 515 nm, respectively. The obtained fluorescence was normalized with total number of cells using an automatic cell counter (Countess™ 3).

Evaluation of reactive oxygen species (ROS). The fluorescent probe DCFH-DA (Invitrogen; Thermo Fisher Scientific, Inc.) was used to monitor ROS. Cells were seeded in six-well plates at a density of 10^4 cells/ml and treated with the different compounds for 24 h. After treatments, cells were collected and incubated with 10 μM DCFH-DA in serum-free medium for 30 min at 37˚C. Fluorescence was measured using a microplate fluorimeter FLX-800 (Bio-Tek Instruments, Inc.,) at an excitation and emission wavelength of 485 and 530 nm, respectively. The obtained fluorescence was normalized with total number of cells using an automatic cell counter (Countess™ 3).

Evaluation of lactate dehydrogenase (LDH) activity. Cells were seeded in 24-well plates at a density of 10^4 cells/ml. Determination of LDH activity was accomplished following specifications of the lactic dehydrogenase based *In Vitro* Toxicology Assay kit (cat. no. MAK066; MilliporeSigma). Absorbance was determined using an automatic microplate reader (μQuant; Bio-Tek Instruments, Inc.) at 490 nm and then the obtained data was relativized with total protein concentration.

Western blot analysis. For protein expression analysis, cells were lysed in ice-cold lysis buffer (150 mM NaCl, 1 mM EDTA, 1 mM EGTA, 1% v/v Triton X-100, 2.5 mM sodium pyrophosphate, 1 mM β-glycerophosphate, 1 mM Na3VO4, 1 μg/ml leupeptin, 2 μg/ml aprotinin, 1 μg/ml pep-statin-A, 110 nM NaF, 1 mM PMSF, 20 mM Tris-HCl pH 7.5). Total protein (30 μg) was separated by 10% SDS-polyacrylamide gel electrophoresis and transferred to polyvinylidene difluoride membranes (Amersham Bioscience; Cytiva). Blots were blocked using Pierce Clear Milk Blocking Buffer (cat. no. 13494209; Pierce; Thermo Fisher Scientific, Inc.) for 1 h at room temperature and incubated overnight at 4˚C with appropriate antibodies (Table SI). Immunoreactive polypeptides were visualized after incubation for 1.5 h at room temperature using horseradish peroxidase conjugated secondary antibodies (anti-rabbit or anti-mousse IgG peroxidase conjugated; 1:4,000; cat. no. sc-2357 and sc-516102 respectively; Santa Cruz Biotechnology, Inc.) and enhanced-chemiluminescence detection reagents (Merck Millipore) following manufacturer-supplied protocols. Chemiluminescence signals were acquired using the Odyssey Fc Imaging System equipment (LI-COR Biosciences) and subsequently processed with the Image Studio 5.2 software (LI-COR Biosciences).

Reverse transcription-quantitative PCR (RT-qPCR). Total RNA was extracted from cells using GenElute™ Mammalian Total RNA Miniprep kit (cat. no. RTN70-1KT; MilliporeSigma). cDNA was constructed by reverse-transcribing 1 μg of total RNA using Applied Biosystems™ High-Capacity cDNA Reverse Transcription kit following manufacturer's protocol (cat. no. 4368814, Thermo Fisher Scientific, Inc.). Quantitative analysis of CD133, SOX 2, OCT3/4 and NANOG levels was performed by the SYBR Green real time PCR method using Green PCR Core Reagents in an AB7700 Real-Time System (both from Applied Biosystems; Thermo Fisher Scientific, Inc.). Thermal cycling parameters were as follows: 95˚C for 10 min, followed by 40 cycles of amplification at 95˚C for 15 sec, 55˚C for 30 sec and 72˚C for 30 sec, with a final elongation step at 72˚C for 5 min. The primers used are presented in Table SII. Each sample was tested in triplicate, and relative gene expression data was analyzed by means of the $2^{-\Delta\Delta Cq}$ method (21).

For evaluation of the levels of expression of glucose metabolism-related genes, RNA was converted to cDNA using the RT2 First Strand kit (cat. no. 330404; Qiagen GmbH), and RT-qPCR was performed using the Qiagen Glucose Metabolism RT2 Profiler PCR Array with the RT2 SYBR Green qPCR Mastermix (Qiagen) on an AB7700 Real-Time System (Applied Biosystems; Thermo Fisher Scientific, Inc.). Data analysis was performed as described by the manufacturer.

Statistical analysis. Experiments were repeated at least three times, and data was calculated as the average ± standard error. Significance was tested by unpaired t-test when two groups were compared, while one-way ANOVA followed by a Tukey's post hoc test was used for multiple group comparison, using the software SigmaStat 3.5 (Systat Software, Inc.). $P \leq 0.05$ was considered to indicate a statistically significant difference.

Results

GICs have been reported to differentiate into non-stem differentiated glioma cell under serum culture conditions (22-24). Differences between stem cells and differentiated counterparts were compared in GBM (GBM grade IV) patient-derived neurospheroid cultures, GIC-A and GIC-B (isolated from two different patients). As expected, after 10 days of culture in a serum containing medium, both displayed a differentiated phenotype with an astrocyte-like morphology and numerous processes forming well-delineated bushy territories (Fig. S1A). Moreover, mRNA expression levels of several stem cells' markers including sox2, oct4, nanog and CD133 revealed a decrease after culture in serum-containing medium (Fig. S1B). Decrease of sox2, a transcription factor whose activity has been described to be essential for GBM stem cells (25) was also demonstrated at the protein levels, together with an increase of glial fibrillary acidic protein expression (GFAP)-a marker of differentiation (Fig. S1C).

GICs are dependent on mitochondrial metabolism. Glucose metabolism in GICs remains unclear since both aerobic glycolysis and mitochondrial dependent glucose metabolism have been described in the literature (13). To assess this discrepancy, glucose uptake, mitochondrial membrane potential and LDH activity (main enzyme in the production of lactate during aerobic glycolysis) were evaluated in the present experimental model. A decrease in glucose uptake (Fig. 1A) and a disruption in mitochondrial membrane potential-as determined by rhodamine 123 fluorescence-(Fig. 1B) was found after differentiation of cells (10 days of serum containing-medium incubation), while LDH activity increased under those culture conditions (Fig. 1C). Moreover, a decrease in intracellular ROS (mainly produced in the mitochondria) also occured during differentiation of glioma stem cells (Fig. 1D). The aforementioned data appeared to indicate that under differentiated conditions, GICs change their metabolism, moving from a greater dependence on mitochondria to a greater dependence on aerobic glycolysis. In this sense, the expression of 84 glucose metabolism-related genes was evaluated using the Qiagen Glucose Metabolism RT2 Profiler PCR Array (Fig. 1E); a decrease was demonstrated in the expression of 36 of those genes after differentiation in serum-containing medium, including certain key genes such as hexokinase 2 (HK2) or pyruvate dehydrogenase (PDH). Only one of the studied genes-TPI-, that encodes for the triosephosphate isomerase-one of the key glycolytic enzymes-, demonstrated increased expression in differentiated glioma cells. Downregulation of HK2 and PDH was also confirmed at the protein level (Fig. 1F and G). Although the higher expression of HK2 in GICs may be unexpected, it must be considered that it is not entirely correct to affirm that HK2 is a glycolytic enzyme since, being the enzyme that participates in the first step of the glucose metabolism pathway. Thus, its expression is necessary both in the cells that then shunt metabolites to mitochondria as well as those that shunt metabolites to lactate production.

According to the aforementioned results, disruption of mitochondrial ETC by rotenone resulted in the induction of GICs' cell death with a significantly fewer effect on the population of differentiated cells (Fig. 2A and B). In the same line, inhibition of LDH by oxamate had not a significant effect on GICs while it induced cell death in differentiated cells (Fig. 2A and B). Although the type of cell death induced by the treatments has not been determined, the data are sufficient to reinforce the idea that after differentiation, cells become more dependent on aerobic glycolysis than mitochondrial metabolism. It also has to be noted that the present data appeared to indicate that differentiation with serum can improve the basal survival of cells in culture in one of the GICs (GIC-A). However, the overall results regarding glucose metabolism parameters did not differ between both GICs, indicating that this fact appears to be rather an artifact due to the particularities of primary cell culture. Disruption of ETC by rotenone also resulted in a decrease of self-renewal (Fig. 2C) that associated with a decrease in the expression of the stem cell marker sox2 (Fig. 2D) which has been described to play a key role in GBM cell stemness and tumor propagation (26). Rotenone treatment not only affected stemness but also induced a shift in cellular metabolism with a disruption of mitochondrial membrane potential, as determined by a decrease in Rhodamine 123 fluorescence (Fig. 2E) and a slight but significant increase in LDH activity (Fig. 2F).

Differences in mitochondrial metabolism between GICs and differentiated tumor cells are related to calcium flux. It is well known that calcium uptake by the mitochondria is essential for the activity of dehydrogenases of the Krebs cycle and therefore the production of energy at the mitochondria (27). In this sense, a decrease in the calcium levels inside the mitochondria was identified (Fig. 3A), which can be implicated in the decrease of the mitochondrial activity observed. A decrease in the expression of VDAC, the main carrier of Ca^{2+} in the outer mitochondrial membrane, was also observed after differentiation, which can be responsible of the observed decrease in mitochondrial calcium (Fig. 3B). In addition, treatment of cells with an intracellular calcium chelator, BAPTA, resulted in the induction of cell death in the GICs subpopulation without any effect on their differentiated counterparts (Fig. 3C) and also a decrease in the self-renewal capability of GICs (Fig. 3D), indicating an essential role of cellular calcium flux in the maintenance of GICs.

As previously stated (27), among the numerous functions that calcium plays in the mitochondria is the regulation of the dehydrogenases of the Krebs cycle and therefore it is closely related with cellular energy metabolism. In this regard, it was revealed that disruption of ETC by rotenone in GICs results in a decrease in the mitochondrial calcium levels (Fig. 3E). In the same way, BAPTA treatment, although it was capable of inducing an increase in glucose uptake (Fig. 3F), it also induced a disruption of mitochondrial membrane potential, as determined by a decrease in the Rhodamine 123 fluorescence

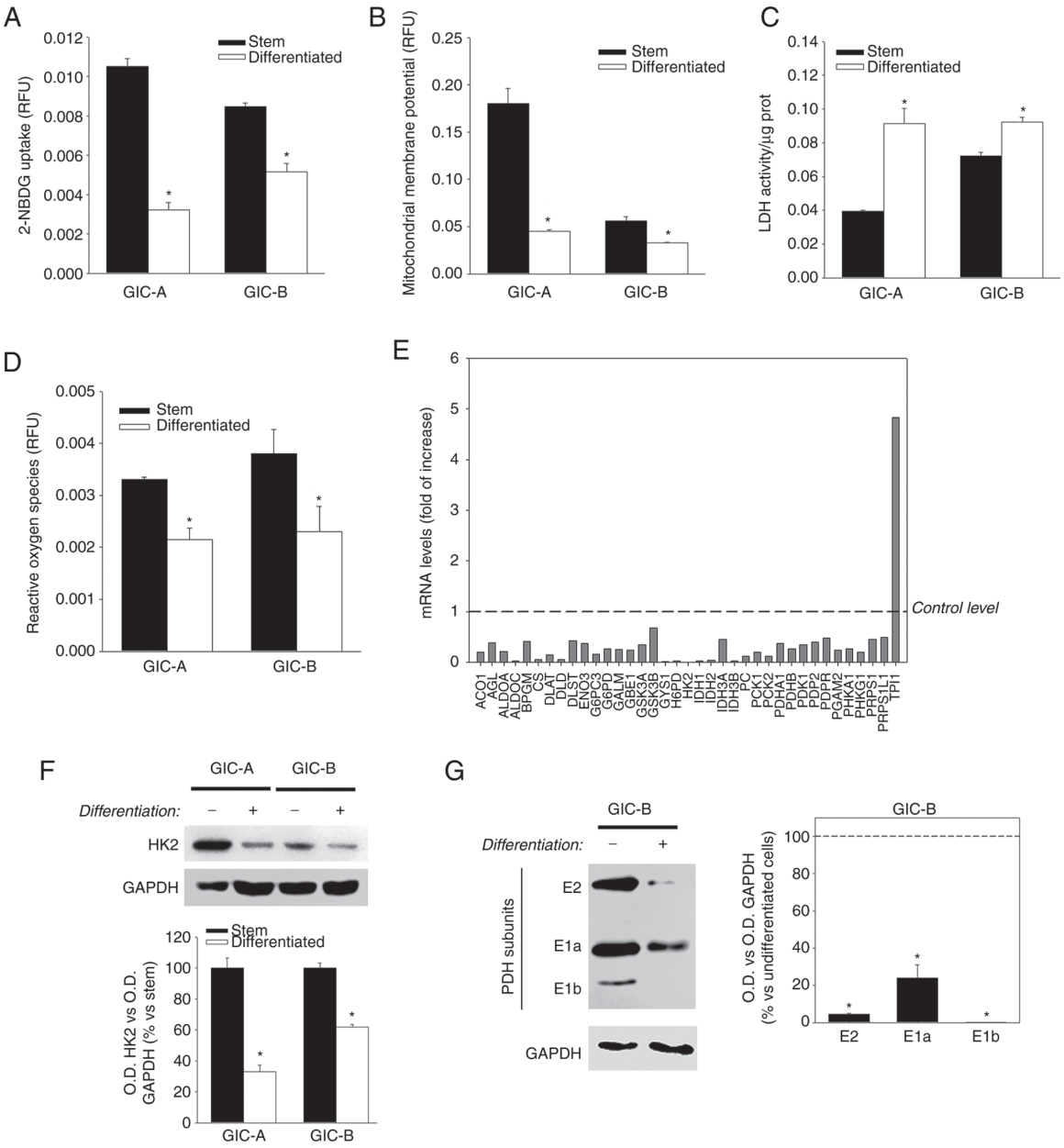

Figure 1. GICs relay more on mitochondrial metabolism that their differentiated progeny. (A) Glucose uptake, (B) mitochondrial membrane potential-as rhodamine 123 fluorescence per cell-, (C) LDH activity and (D) reactive oxygen species were determined in neutrospheres cultures (stem) and their differentiated counterpart. (E) mRNA expression levels of glucose metabolism related genes in differentiated vs. stem cells determined by reverse transcription-quantitative PCR. Only those genes with a decrease in their expression of at least half or an increase in their expression of at least double have been represented. Dashed line represents the level of expression of stem cell. (F and G) Representative blot showing the protein expression of HK2 and PDH (E1a, E1b and E2 subunits) in both stem cells and their differentiated counterparts. GAPDH expression has been used as loading control. Dashed line represents levels of expression of stem cells. *P≤0.05 vs. stem. GICs, glioma initiating cells; LDH, lactate dehydrogenase; ACO1, aconitase 1, soluble; AGL, amylo-alpha-1, 6-glucosidase, 4-alpha-glucanotransferase; ALDOA, aldolase A, fructose-bisphosphate; ALDOC, aldolase C, fructose-bisphosphate; BPGM, 2,3-bisphosphoglycerate mutase; CS, citrate synthase; DLAT, dihydrolipoamide S-acetyltransferase; DLD, dihydrolipoamide dehydrogenase; DLST, dihydrolipoamide S-succinyl-transferase (E2 component of 2-oxo-glutarate complex); ENO3, enolase 3 (beta, muscle); G6PC3, glucose 6 phosphatase, catalytic, 3; G6PD, glucose-6-phosphate dehydrogenase; GALM, galactose mutarotase (aldose 1-epimerase); GBE1, glucan (1,4-alpha-), branching enzyme 1; GSK3A, glycogen synthase kinase 3 alpha; GSK3B, glycogen synthase kinase 3 beta; GYS1, glycogen synthase 1 (muscle); H6PD, hexose-6-phosphate dehydrogenase (glucose 1-dehydrogenase); HK2, hexokinase 2; IDH1, isocitrate dehydrogenase 1 (NADP+), soluble; IDH2, isocitrate dehydrogenase 2 (NADP+), mitochondrial; IDH3A, isocitrate dehydrogenase 3 (NAD+) alpha; IDH3B, isocitrate dehydrogenase 3 (NAD+) beta; PC, pyruvate carboxylase; PCK1, phos-phoenolpyruvate carboxykinase 1 (soluble); PCK2, phosphoenolpyruvate carboxykinase 2 (mitochondrial); PDHA1, pyruvate dehydrogenase (lipoamide) alpha 1; PDHB, pyruvate dehydrogenase (lipoamide) beta; PDK1, pyruvate dehydrogenase kinase, isozyme 1; PDP2, pyruvate dehydrogenase phosphatase catalytic subunit 2; PDPR, pyruvate dehydrogenase phosphatase regulatory subunit; PGAM2, phosphoglycerate mutase 2 (muscle); PHKA1, phosphorylase kinase, alpha 1 (muscle); PHKG1, phosphorylase kinase, gamma 1 (muscle); PRPS1, phosphoribosyl pyrophosphate synthetase 1; PRPS1L1, phosphoribosyl pyrophosphate synthetase 1-like 1; TPI1, triosephosphate isomerase 1.

in GICs (Fig. 3G), reinforcing the idea of a close relationship between calcium flux to the mitochondria and glucose metabolism in GICs.

ER-mitochondria interaction is determinant for metabolism and maintenance of GICs. In agreement with data obtained after BAPTA treatment, incubation of GICs with thapsigargin,

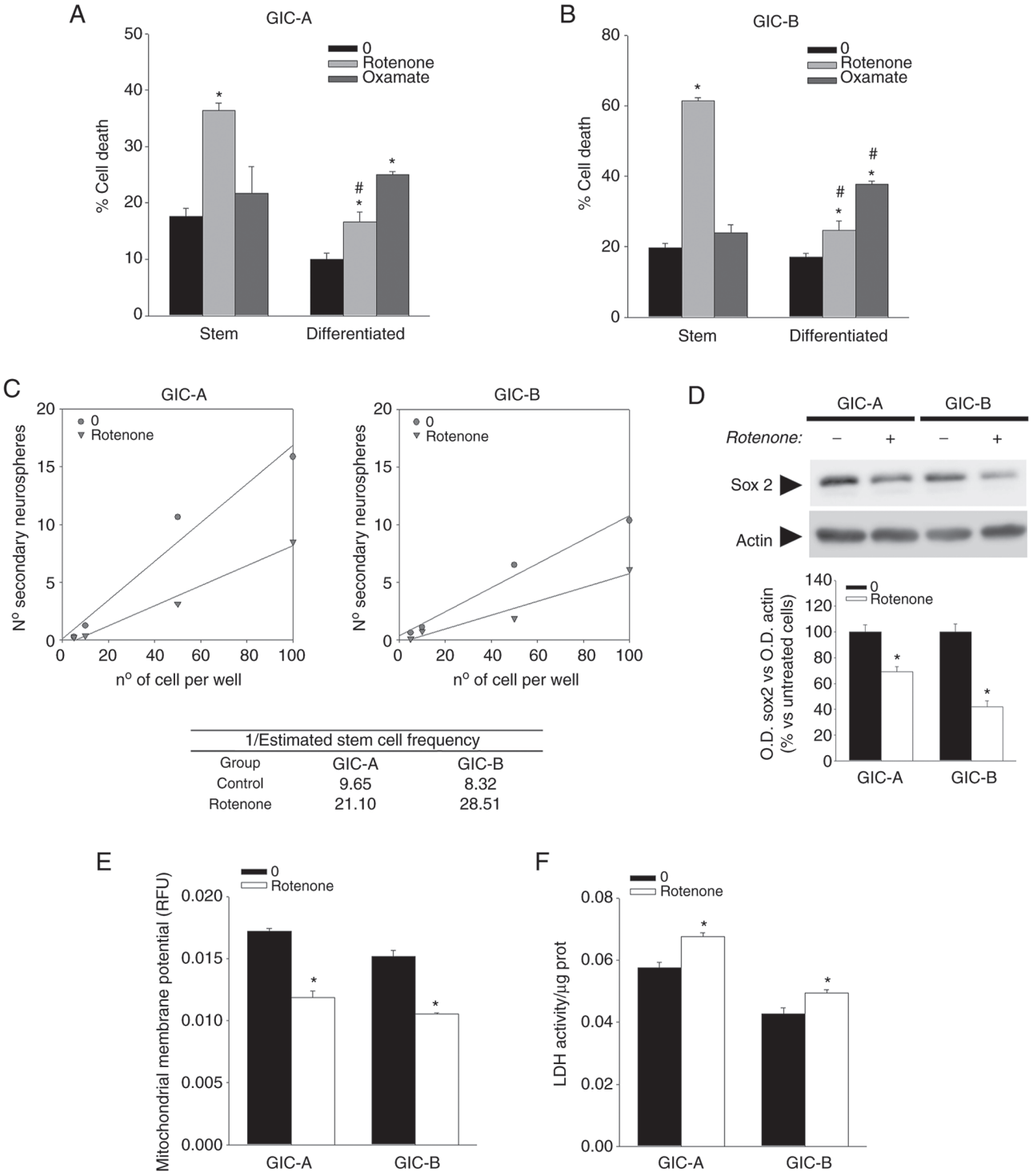

1/Estimated stem cell frequency		
Group	GIC-A	GIC-B
Control	9.65	8.32
Rotenone	21.10	28.51

Figure 2. Mitochondrial metabolism is essential for GICs' maintenance. (A and B) Cell death was determined after treatment of stem cells and their differentiated counterparts with 500 nM rotenone (electron transport chain inhibitor) or 20 mM oxamate (lactate dehydrogenase inhibitor) for 48 h. (C) *In vitro* self-renewal limiting dilution assay after overnight treatment with 500 nM rotenone was performed for the two different GIC neurosphere cultures. After treatment, cells were seeded at dilutions that ranged from 100 to 1 cell/well and the number of cells that are needed to form a secondary neurosphere formation was determined after 10 days in culture. Estimated stem cell frequency for each experimental group was determined using a web-based tool (ELDA, http://bioinf.wehi.edu.au/software/elda/). (D) Representative blot showing the decrease in the protein expression of sox2 after treatment of GICs neurospheres with 500 nM rotenone for 24 h. Actin expression has been used as loading control. (E) Mitochondrial membrane potential-as rhodamine 123 fluorescence per cell and (F) LDH activity were determined after treatment of GIC neurospheres with 500 nM rotenone for 24 h. $^{*}P\leq0.05$ vs. untreated cells and $^{\#}P\leq0.05$ vs. stem cells. GICs, glioma initiating cells.

a potent inhibitor of the ion transport activity of sarco/ER Ca^{2+}-ATPases (SERCA), that disrupt calcium homeostasis at the ER-the main calcium reservoir in the cell-also induced cell death (Fig. 4A). Moreover, thapsigargin treatment of GICs also induced a decrease in mitochondrial calcium (Fig. 4B) that was accompanied by an increase in LDH activity (Fig. 4C) suggesting that disruption of calcium homeostasis at the ER results in an alteration of mitochondrial calcium that is

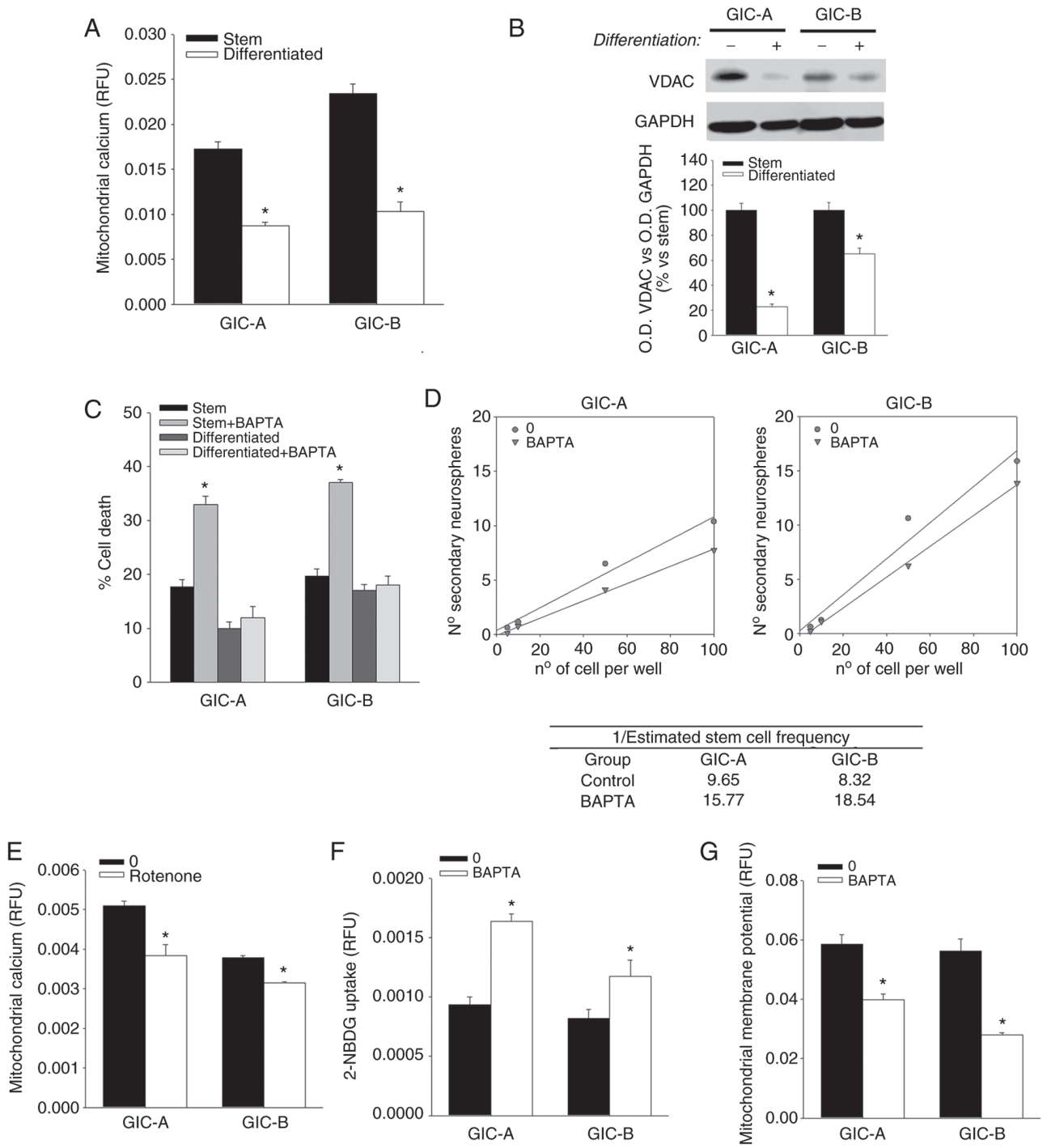

Figure 3. Calcium flux and mitochondrial metabolism are close related in GICs. (A) Mitochondrial calcium levels were determined in neurosphere cultures and their differentiated counterparts. (B) Representative blot showing the decrease in the protein expression of VDAC after GICs differentiation. GAPDH expression was used as loading control. (C) Cell death was determined after treatment of GIC neurospheres and their differentiated counterparts with 10 μM BAPTA (intracellular calcium chelator) for 48 h. (D) *In vitro* self-renewal limiting dilution assay after overnight treatment with 10 μM was performed for the two different GIC neurospheres cultures. After treatment, cells were seeded at dilutions that ranged from 100 to 1 cell/well and the number of cells that were needed to form a secondary neurosphere formation was determined after 10 days in culture. Estimated stem cell frequency for each experimental group was determined using a web-based tool (ELDA, http://bioinf.wehi.edu.au/software/elda/). (E) Mitochondrial calcium determined after treatment of GIC neurospheres with 500 nM rotenone for 24 h. (F) Glucose uptake and (G) mitochondrial membrane potential were determined in GIC neurospheres after treatment with 10 μM BAPTA for 24 h. *P≤0.05 vs. stem or untreated cells. GICs, glioma initiating cells; VDAC, voltage-dependent anionic channel.

probably related to a swift from mitochondrial metabolism to aerobic glycolysis.

Since thapsigargin, due to its action on SERCA, is commonly used as an ER stress inducer, these results also pointed out the possible relevance of ER homeostasis in GICs maintenance. Interestingly, a decrease was found in the expression of Bip, a central regulator for ER stress (28), after differentiation of serum-induced GICs (Fig. 4D). Moreover, a decrease was also identified in the expression of endoplasmic reticulum oxidoreductase 1 alpha (ERO1α), protein disulfide

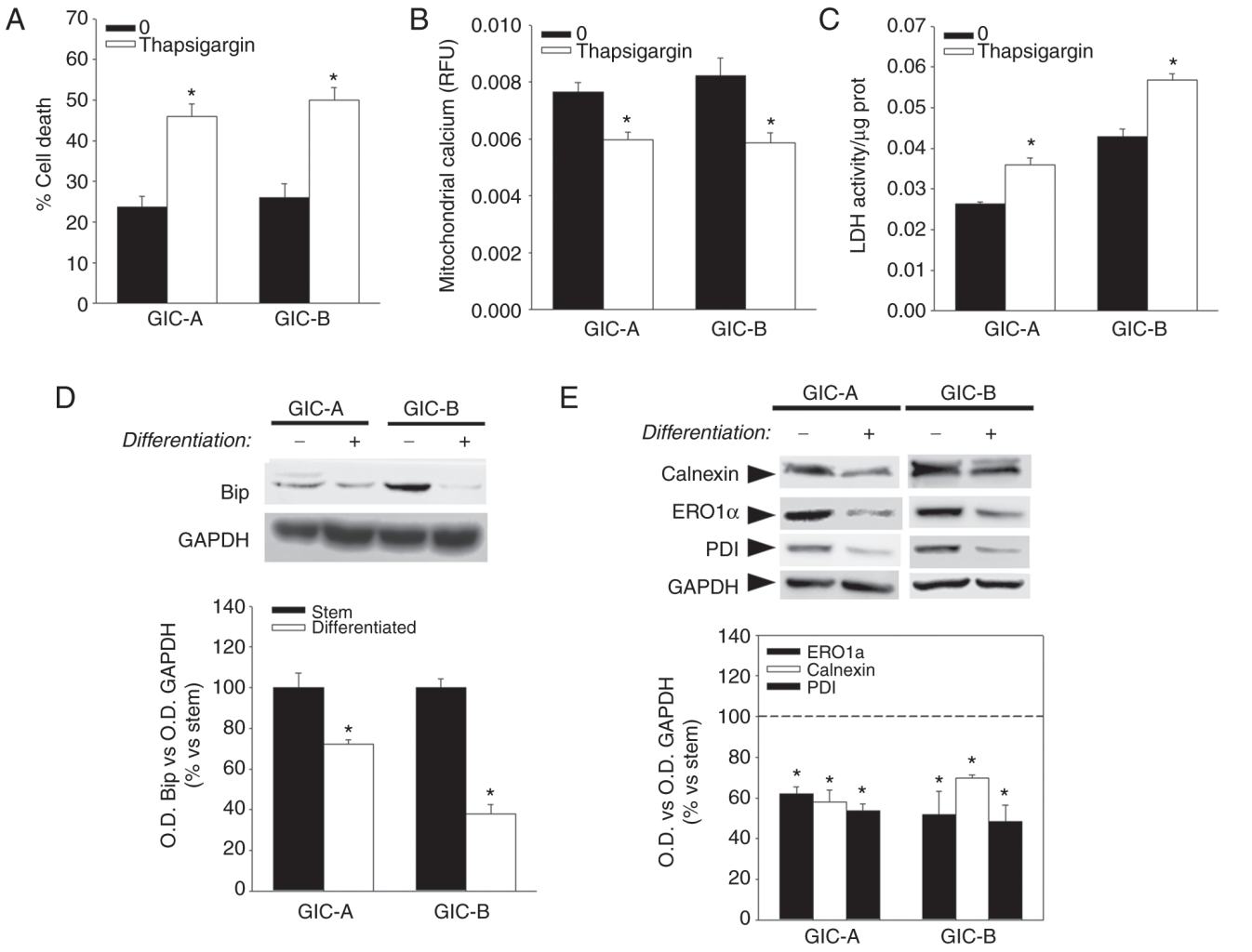

Figure 4. Calcium homeostasis plays a key role in maintenance and metabolism of GICs. (A) Cell death, (B) mitochondrial calcium and (C) LDH activity determined after treatment of GIC neurospheres with 5 μM thapsigargin for 48 h. (D) Representative blot showing the decrease in the protein expression of Bip after GICs' differentiation. GAPDH expression has been used as loading control. (E) Representative blot showing the expression levels of ER-related proteins (ERO1α, PDI, calnexin and IP3R) after GICs' differentiation. GAPDH expression has been used as loading control. Dashed line represents levels of expression of GIC neurospheres (stem). *P≤0.05 vs. stem or untreated cells. GICs, glioma initiating cells; LDH, lactate dehydrogenase.

isomerase (PDI) and the ER calcium-binding protein calnexin (Fig. 4E) under differentiation culture conditions. ERO1α and PDI have been described to play a crucial role in ER calcium homeostasis and calcium transfer to the mitochondria (29).

The use of modulators of ER activity also reflected differences between GIC and their differentiated counterparts. Thus, treatment of cells with tunicamycin, another ER stress inducer, also resulted in death of GICs without any cytotoxic effect in their differentiated counterparts cells (Fig. 5A), while treatment of cells with the chemical chaperone 4-phenyl butyric acid, that attenuates ER stress, had no cytotoxic effects on GICs or differentiated (data not shown). Moreover, tunicamycin treatment also induced an increase in glucose uptake that associated with a decrease in rhodamine 123 fluorescence (Fig. 4B and C), as it was observed for treatment with BAPTA, indicating that this glucose is probably derived to a metabolic pathway other than mitochondrial. Tunicamycin treatment also induced a decrease in self-renewal capability in GICs (Fig. 5D).

Collectively, the aforementioned data suggested an important role of ER in the regulation of calcium flux and glucose metabolism in GICs. It is important to note that mitochondrial calcium influx represents one of the main functions of ER-mitochondria connections through MERCS (16). In this regard, it is well known that the tight connection between VDAC1 and the IP3R through the chaperone GPR75 represents the main mechanism of ER to mitochondria calcium influx. Of interest, although an increase in the expression of IP3R was identified after serum-induced differentiation (Fig. 6A), a decrease was also observed in the expression of GRP75, both at mRNA (Fig. 6B) and protein levels (Fig. 6A), in addition to the decrease in VDAC expression that was already observed. The use of a chemical GRP75 inhibitor, MKT-077 revealed that inhibition of this protein was toxic for GICs (Fig. 6C). MKT-077 treatment also induced a disruption of the mitochondrial membrane potential on GICs, as reflected by a decrease in rhodamine 123 fluorescence (Fig. 6D), reinforcing the idea of a key function of these ER-mitochondria connections in the regulation of GICs' metabolism; MKT-077 also enhanced the effect of temozolomide on GICs (Fig. 6E) -current treatment for malignant gliomas-opening the possibility of using this protein as a target for the development of new therapies.

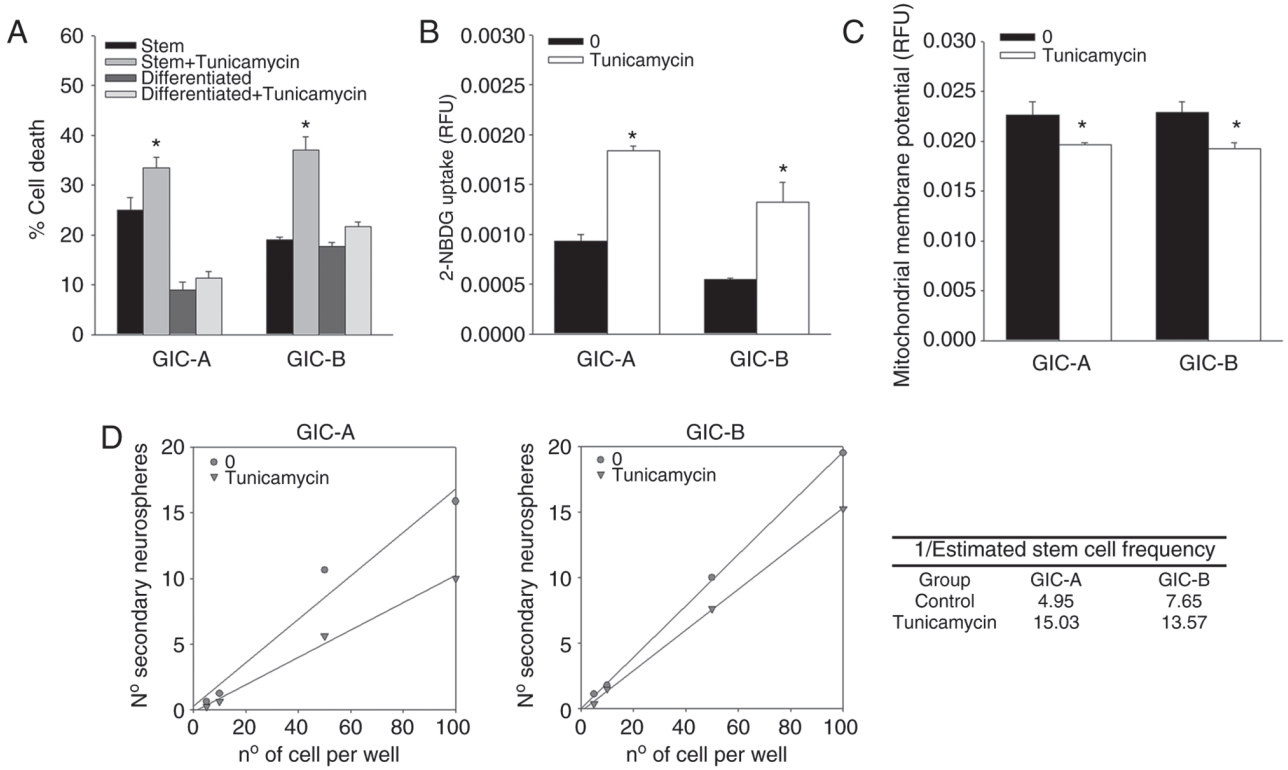

1/Estimated stem cell frequency		
Group	GIC-A	GIC-B
Control	4.95	7.65
Tunicamycin	15.03	13.57

Figure 5. ER homeostasis plays a key role in GICs maintenance and metabolism. (A) Cell death was determined after treatment of GIC neurospheres and their differentiated counterparts with 500 ng/ml tunicamycin (ER stress inducer) for 48 h. (B) Glucose uptake and (C) mitochondrial membrane potential were determined in GIC neurospheres after treatment with 500 ng/ml tunicamycin for 24 h. (D) *In vitro* self-renewal limiting dilution assay after overnight treatment with 500 ng/ml tunicamycin was performed for the two different GIC neurospheres cultures. After treatment, cells were seeded at dilutions that ranged from 100 to 1 cell/well and the number of cells that are needed to form a secondary neurosphere formation was determined after 10 days in culture. Estimated stem cell frequency for each experimental group was determined using a web-based tool (ELDA, http://bioinf.wehi.edu.au/software/elda/). *P≤0.05 vs. its own control (stem or differentiated counterpart) or untreated cells. ER, endoplasmic reticulum; GICs, glioma initiating cells.

Discussion

The present study indicated that GBM cells are heterogeneous in their metabolic phenotypes, being GICs more dependent on oxidative phosphorylation (OXPHOS) at the mitochondria than their differentiated progeny. This distinct metabolic state appears to be related to ER homeostasis that affects functioning of ER-mitochondrial contact sites. Although the impact of the ER-mitochondrial contact sites on metabolism has not been evaluated in normal stem cells from same patients (since they cannot be isolated from tumor tissue) or in commercial cell lines (since there are no commercial cell lines of human glial precursors derived from adults, to the best of our knowledge), the present study attempted to establish differences between two different tumor subpopulations within the tumor rather to compare between normal and tumor cells.

Genetic alterations and environmental modifications, such as hypoxia, converge in one of the traits that define tumor cells and that are in the spotlight for the design of new therapeutic strategies. In fact, metabolic adaptation is considered one of the hallmarks of cancer (8), being aerobic glycolysis or the Warburg effect the main change in cancer cells. Thus, cancer cells move from OXPHOS as a way of obtaining their energy towards lactate production, even at normal oxygen concentrations. However, there are relatively few studies and quite a few discrepancies in relation to the metabolic pathways used by CSCs in general and GICs in particular. Some studies indicated that CSCs have a distinctive metabolic phenotype compared with tumor bulk cells, although there is so far no consensus on this. Thus, both the preferential use of aerobic glycolysis and the mitochondrial oxidative metabolism have been described (13). Trying to address this discrepancy, the present results demonstrated that GICs use mitochondrial metabolism preferably and that this metabolic pathway decreases after differentiation to tumor bulk cells by incubation in a medium with serum for 10 days. Despite measurements have not been performed on differentiated cells isolated directly from the patient tissue due to the GICs isolation protocol, differentiation in serum is a well-established protocol in the literature. Although a decrease was found in glucose uptake-which can be considered contrary to what happens in the Warburg effect-glioma cells increased LDH activity in association to an alteration of mitochondrial activity when differentiated. This change in mitochondrial activity was accompanied by a decrease in intracellular ROS. In this sense, although ROS produced by mitochondria were not directly evaluated, it is well established that the mitochondria, through the ETC, is the main producer of ROS inside the cell. Moreover, GICs were more sensitive to the inhibition of ETC by rotenone and less sensitive to LDH inhibition by oxamate compared with their differentiated counterparts. These results are in consistency with previous studies that described a decrease of stemness in CSCs from different tumors, such as breast or prostate cancer, after inhibition of complex I of the ETC (30,31). It must be

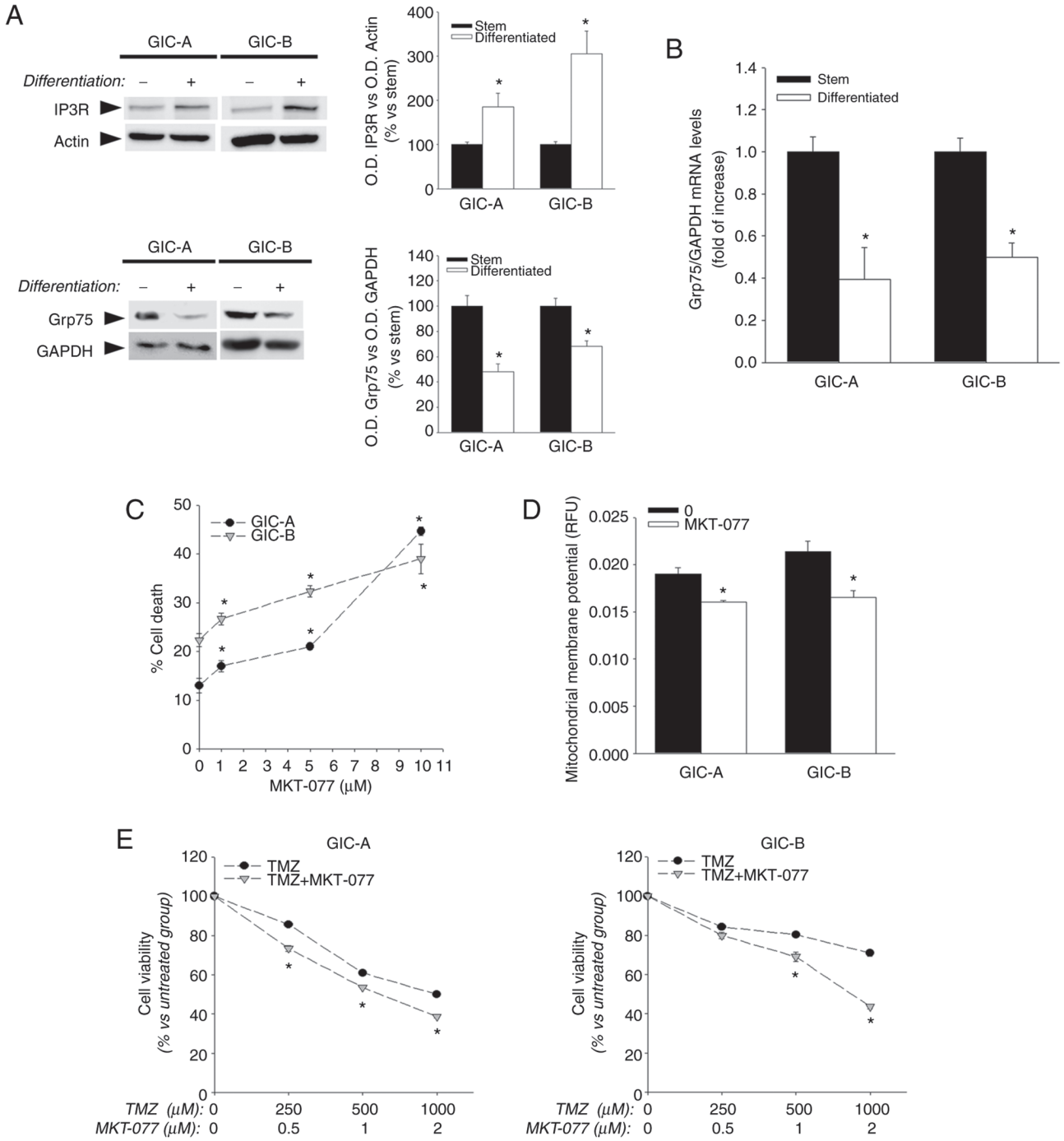

Figure 6. Grp75 is essential for maintenance of GICs. (A) Representative blot showing the protein expression of IP3R and Grp75 after GICs differentiation. (B) Decrease of mRNA expression of Grp75 after GICs differentiation. (C) Cell death was determined after treatment of GIC neurosphere cultures and their differentiated counterparts with the Grp75 inhibitor MKT-077 (1 to 10 μM) for 48 h. (D) Mitochondrial membrane potential was determined in GIC neurosphere cultures after treatment with 1 μM MKT-077 for 24 h. (E) Effect of combination of temozolomide and MKT-077 (500:1 constant ratio) on GIC neurosphere cultures cell viability as determined by MTT assay. *P≤0.05 vs. stem or untreated cells or temozolomide alone. GICs, glioma initiating cells.

considered that several studies carried out on different types of tumors appear to indicate that the metabolic phenotype of CSCs can be modified depending on the state of differentiation, tumor microenvironment, or expression of certain oncogenes, which could explain divergence results already published, even within the same tumor type (32).

Mitochondrial bioenergetics is largely controlled by extra mitochondrial events whose activity are frequently altered in cancer such as calcium homeostasis. Mitochondria can act both as a reservoir of Ca^{2+} and as an effector that utilize Ca^{2+} to regulate cell survival, proliferation, redox state and metabolic changes (33). This mitochondrial Ca^{2+} homeostasis requires an efficient interplay between ER, where most intracellular Ca^{2+} is stored, and mitochondria through MERCS (34,35). Thus, controlled raises in matrix Ca^{2+} concentration have important metabolic effects, as Ca^{2+} enhances the activity of mitochondrial dehydrogenases of the TCA cycle, IDH and αKGDH, and of PDH (34). The

decrease in mitochondrial calcium that was observed after differentiation of GICs could be responsible, at least in part, for the distinct metabolic phenotype observed between GICs and their differentiated progeny. In fact, it was found that alterations in calcium homeostasis using calcium chelators not only resulted toxic for the subpopulation of GICs, decreasing also self-renewal capacity, but also induced changes in glucose metabolism such as an increase in glucose uptake and a disruption in mitochondrial membrane potential. Although these results may appear contradictory, the fact that an increase in glucose uptake in GICs does not correlate to an increase in mitochondrial activity could be explained by the fact that use of that glucose may be derived to other metabolic pathways. As an example, it has been described that quiescent breast CSCs have a high metabolic rate of the pentose phosphate pathway, which favors the generation of reducing power (NADPH), essential for the maintenance of the state cellular redox (36).

The decrease in the expression of Bip, central regulator of ER stress responses, after differentiation of GICs, together with the fact that similar effects were observed in cell viability, self-renewal and glucose metabolism when using ER stress inducers compared with calcium chelators, appears to indicate that ER homeostasis also plays a key role in GICs' maintenance and metabolism. Moreover, a decrease was also identified in the expression of ERO1α, PDI and the ER calcium-binding protein calnexin after differentiation. ERO1α-PDI have been described to be enriched at the MERCS interface and to play a crucial role in calcium flux from ER to mitochondria. Thus, downregulation of Ero1α inhibits mitochondrial Ca^{2+} fluxes and modifies the activity of mitochondrial Ca^{2+} uniporters (29).

In this sense, it is important to note that mitochondrial calcium influx represents one of the main functions of ER-mitochondria connections (16), being the IP3Rs-Grp75-VDACs complex the basis for the mitochondrial Ca^{2+} transfer in MERCS (37). In this regard, a decrease was revealed in VDAC expression in differentiated cells that can be responsible for the observed decrease in mitochondrial calcium level. The relevance of VDAC expression in GBM has been already described. Thus, inhibition of VDAC expression by siRNA has been described to inhibit GBM growth and to reduce angiogenesis, invasiveness and stemness (38). A decrease was also demonstrated in the expression of Grp75, also known as mortalin, after differentiation of GICs. This protein has been described to be enriched in a large variety of cancers and it is also considered to act as a regulatory factor in the maintaining the stemness of the CSCs (39). Thus, it has been reported that mortalin is able to upregulate the activity of some CSCs signaling pathways such as the Wnt/GSK3β/β-catenin in breast and colorectal cancer (40,41). Moreover, upregulation of mortalin expression in correlation with malignant progression in brain tumors has been described several years ago (42). The use of a chemical Grp75 inhibitor revealed an essential role of this protein in GICs' survival, chemoresistance and mitochondrial metabolism maintenance. It is well known that GICs resist current treatments and repopulate the tumor being responsible for patient death. Thus, the greater proportion of GICs, the higher tumor aggression and poorer prognosis as current therapies show poor efficacy against GICs. Understanding the differences between both tumor subpopulation can help to move cancer therapy towards less conventional but more efficient approaches. Combination of Grp75 inhibitor and temozolomide, current chemotherapeutic treatment for malignant gliomas, resulted in an increased GICs' death, suggesting that Grp75, and therefore the ER-mitochondria connection through the IP3Rs-Grp75-VDACs complex, is also important for chemoresistance of this CSC subpopulation and could perhaps be taken into account as a target for the development of new and more efficient therapies.

Acknowledgements

The authors would like to acknowledge support from the BioISI/FCUL Microscopy Facility, a node of the Portuguese Platform of BioImaging (PPBI-POCI-01-0145-FEDER-022122).

Funding

The present study was supported by the UIDB/04046/2020 and UIDP/04046/2020, and individual grants (grant nos. PTDC/MED-NEU/31417/2017 and PTDC/FIS-MAC/2741/2021) through Fundação para a Ciência e Tecnologia (FCT, Portugal). It was also supported by the Spaniard Association Against Cancer (AECC; grant no. SV-19-AECC-FPI) and the Consejería de Economía y Empleo del Principado de Asturias (FICYT; grant no. Severo-Ochoa BP20-073) fellowships. IUOPA is supported by the 'Obra Social Cajastur' and the Government of the Principality of Asturias.

Availability of data and materials

The datasets used and/or analyzed during the current study are available from the corresponding author upon reasonable request.

Authors' contributions

IA, CR and VM conceptualized the present study. MTC, AMSS, NPM and MAAV performed laboratory experiments. VM supervised the study. MTC performed data visualization. IA, CR and VM wrote the original draft. FH, JRB contributed to the interpretation of the data and reviewing the manuscript. MTC and VM confirm the authenticity of all the raw data. All authors read and approved the final manuscript.

Ethics approval and consent to participate

The present study was conducted in accordance with the Declaration of Helsinki and was approved (approval no. 2021.008; approved on January 22nd, 2021) by the Clinical Research Ethics Committee of the Principality of Asturias (Oviedo, Spain). Written informed consent was obtained by all patients who participated in the present study.

Patient consent for publication

Not applicable.

Competing interests

The authors declare that they have no competing interests.

References

1. Hussain SF, Yang D, Suki D, Aldape K, Grimm E and Heimberger AB: The role of human glioma-infiltrating Mi-croglia/Macrophages in mediating antitumor immune responses. Neuro Oncol 8: 261-279, 2006.
2. Charalambous C, Chen T and Hofman FM: Characteristics of tumor-associated endothelial cells derived from glioblastoma multiforme. Neurosurg Focus 20: E22, 2006.
3. Castro MG, Cowen R, Williamson IK, David A, Jimenez-Dalmaroni MJ, Yuan X, Bigliari A, Williams JC, Hu J and Lowenstein PR: Current and future strategies for the treatment of malignant brain tumors. Pharmacol Ther 98: 71-108, 2003.
4. Binello E and Germano IM: Targeting glioma stem cells: A novel framework for brain tumors. Cancer Sci 102: 1958-1966, 2011.
5. Suvà ML, Rheinbay E, Gillespie SM, Patel AP, Wakimoto H, Rabkin SD, Riggi N, Chi AS, Cahill DP. Nahed BV, *et al*: Reconstructing and reprogramming the tumor-propagating potential of glioblastoma stem-like cells. Cell 157: 580-594, 2014.
6. Bao S, Wu Q, McLendon RE, Hao Y, Shi Q, Hjelmeland AB, Dewhirst MW, Bigner DD and Rich JN: Glioma stem cells promote radioresistance by preferential activation of the DNA damage response. Nature 444: 756-760, 2006.
7. Menendez JA, Corominas-Faja B, Cuyàs E and Alarcón T: Metabostemness: Metaboloepigenetic reprogramming of cancer stem-cell functions. Oncoscience 1: 803-806, 2014.
8. Hanahan D and Weinberg RA: Hallmarks of cancer: The next generation. Cell 144: 646-674, 2011.
9. Vander Heiden MG, Cantley LC and Thompson CB: Understanding the Warburg Effect: The metabolic requirements of cell proliferation. Science 324: 1029-1033, 2009.
10. Brand KA and Hermfisse U: Aerobic glycolysis by proliferating cells: A protective strategy against reactive oxygen species. FASEB J 11: 388-395, 1997.
11. Menendez JA, Joven J, Cufí S, Corominas-Faja B, Oliveras-Ferraros C, Cuyàs E, Martin-Castillo B, Lopez-Bonet E, Alarcón T and Vazquez-Martin A: The warburg effect version 2.0: Metabolic reprogramming of cancer stem cells. Cell Cycle 12: 1166-1179, 2013.
12. Vlashi E, Lagadec C, Vergnes L, Matsutani T, Masui K, Poulou M, Popescu R, Della Donna L, Evers P, Dekmezian C, *et al*: Metabolic state of glioma stem cells and nontumorigenic cells. Proc Natl Acad Sci USA 108: 16062-16067, 2011.
13. Martin V, Turos-Cabal M, Sanchez-Sanchez AM and Rodríguez C: Metabolism-redox interplay in tumor stem cell signaling. Handbook of oxidative stress in cancer: Mechanistic Aspects, pp1-22, 2021.
14. Lin H, Patel S, Affeck VS, Wilson I, Turnbull DM, Joshi AR, Maxwell R and Stoll EA: Fatty acid oxidation is Re-quired for the respiration and proliferation of malignant glioma cells. Neuro Oncol 19: 43-54, 2017.
15. Wang M and Kaufman RJ: The impact of the endoplasmic reticulum protein-folding environment on cancer development. Nat Rev Cancer 14: 581-597, 2014.
16. Rowland AA and Voeltz GK: Endoplasmic reticulum-mitochondria contacts: Function of the junction. Nat Rev Mol Cell Biol 13: 607-625, 2012.
17. Cardenas C, Miller RA, Smith I, Bui T, Molgo J, Müller M, Vais H, Cheung KH, Yang J, Parker I, *et al*: Essential regulation of cell bioenergetics by constitutive InsP3 Receptor Ca2+ Transfer to Mitochondria. Cell 142: 270-283, 2010.
18. Arismendi-Morillo G, Castellano-Ramírez A and Seyfried TN: Ultrastructural characterization of the mitochon-dria-associated membranes abnormalities in human astrocytomas: Functional and therapeutics implications. Ultrastruct Pathol 41: 234-244, 2017.
19. Galli R, Binda E, Orfanelli U, Cipelletti B, Gritti A, de Vitis S, Fiocco R, Foroni C, Dimeco F and Vescovi A: Isolation and Characterization of Tumorigenic, Stem-like Neural Precursors from Human Glioblastoma. Cancer Res 64: 7011-7021, 2004.
20. Singh SK, Hawkins C, Clarke ID, Squire JA, Bayani J, Hide T, Henkelman RM, Cusimano MD and Dirks PB: Identification of human brain tumour initiating cells. Nature 432: 396-401, 2004.
21. Livak KJ and Schmittgen TD: Analysis of relative gene expression data using real-time quantitative PCR and the 2(-Delta Delta C(T)) method. Methods 25: 402-408, 2001.
22. Zheng H, Ying H, Wiedemeyer R, Yan H, Quayle SN, Ivanova EV, Paik JH, Zhang H, Xiao Y, Perry SR, *et al*: PLAGL2 regulates Wnt signaling to impede differentiation in neural stem cells and gliomas. Cancer Cell 17: 497-509, 2010.
23. Hong X, Chedid K and Kalkanis SN: Glioblastoma cell line-derived spheres in serum containing medium versus serum-free medium: A comparison of cancer stem cell properties. Int J Oncol 41: 1693-1700, 2012.
24. Kim EJ, Jin X, Kim OR, Ham SW, Park SH and Kim H: Glioma stem cells and their non-stem differentiated glioma cells exhibit differences in mitochondrial structure and function. Oncol Rep 39: 411-416, 2018.
25. Gangemi RM, Griffero F, Marubbi D, Perera M, Capra MC, Malatesta P, Ravetti GL, Zona GL, Daga A and Corte G: SOX2 silencing in glioblastoma tumor-initiating cells causes stop of proliferation and loss of tumorigenicity. Stem Cells 27: 40-48, 2009.
26. Lopez-Bertoni H, Johnson A, Rui Y, Lal B, Sall S, Malloy M, Coulter JB, Lugo-Fagundo M, Shudir S, Khela H, *et al*: Sox2 induces glioblastoma cell stemness and tumor propagation by repressing TET2 and deregulating 5hmC and 5mC DNA modifications. Signal Transduct Target Ther 7: 37, 2022.
27. Contreras L, Drago I, Zampese E and Pozzan T: Mitochondria: The calcium connection. Biochim Biophys Acta 1797: 607-618, 2010.
28. Kopp MC, Larburu N, Durairaj V. Adams CJ and Ali MMU: UPR Proteins IRE1 and PERK Switch BiP from Chaperone to ER Stress Sensor. Nat Struct Mol Biol 26: 1053-1062, 2019.
29. Anelli T, Bergamelli L, Margittai E, Rimessi A, Fagioli C, Malgaroli A, Pinton P, Ripamonti M, Rizzuto R and Sitia R: Ero1α Regulates Ca2+ fluxes at the endoplasmic reticulum-mitochondria interface (MAM). Antioxid Redox Signal 16: 1077-1087, 2012.
30. Jung JW, Park SB, Lee SJ, Seo MS, Trosko JE and Kang KS: Metformin represses self-renewal of the human breast carcinoma stem cells via inhibition of estrogen receptor-mediated OCT4 Expression. PLoS One 6: e28068, 2011.
31. Mayer MJ, Klotz LH and Venkateswaran V: Metformin and prostate cancer stem cells: A novel therapeutic target. Prostate Cancer Prostatic Dis 18: 303-309, 2015.
32. Snyder V, Reed-Newman TC, Arnold L, Thomas SM and Anant S: Cancer stem cell metabolism and potential therapeutic targets. Front Oncol 8: 203, 2018.
33. Cannino G, Ciscato F, Masgras I, Sánchez-Martín C and Rasola A: Metabolic plasticity of tumor cell mitochondria. Front Oncol 8: 333, 2018.
34. Filadi R and Pozzan T: Generation and functions of second messengers microdomains. Cell Calcium 58: 405-414, 2015.
35. Tarasov AI, Griffiths EJ and Rutter GA: Regulation of ATP production by mitochondrial Ca(2+). Cell Calcium 52: 28-35, 2012.
36. Debeb BG, Lacerda L, Larson R, Wolfe AR, Krishnamurthy S, Reuben JM, Ueno NT, Gilcrease M and Woodward WA: Histone deacetylase inhibitor-induced cancer stem cells exhibit high pentose phosphate pathway metabolism. Oncotarget 7: 28329-28339, 2016.
37. Wang N, Wang C, Zhao H, He Y, Lan B, Sun L and Gao Y: The MAMs structure and its role in cell death. Cells 10: 657, 2021.
38. Arif T, Krelin Y, Nakdimon I, Benharroch D, Paul A, Dadon-Klein D and Shoshan-Barmatz V: VDAC1 is a molecular target in glioblastoma, with its depletion leading to reprogrammed metabolism and reversed oncogenic properties. Neuro Oncol 19: 951-964, 2017.
39. Yun CO, Bhargava P, Na Y, Lee JS, Ryu J, Kaul SC and Wadhwa R: Relevance of mortalin to cancer cell stemness and cancer therapy. Sci Rep 7: 42016, 2017.
40. Wei B, Cao J, Tian JH, Yu CY, Huang Q, Yu JJ, Ma R, Wang J, Xu F and Wang LB: Mortalin maintains breast cancer stem cells stemness via activation of Wnt/GSK3β/β-Catenin signaling pathway. Am J Cancer Res 11: 2696-2716, 2021.
41. Xu M, Zhang Y, Cui M, Wang X and Lin Z: Mortalin contributes to colorectal cancer by promoting proliferation and epithelial-mesenchymal transition. IUBMB Life 72: 771-781, 2020.
42. Takano S, Wadhwa R, Yoshii Y, Nose T, Kaul SC and Mitsui Y: Elevated levels of mortalin expression in human brain tumors. Exp Cell Res 237: 38-45, 1997.